Nuclear Engineering and Technology 51 (2019) 518–525

Contents lists available at ScienceDirect

Nuclear Engineering and Technology

journal homepage: www.elsevier.com/locate/net

Original Article

Impact of thermal and chemical treatment on the mechanical properties of E110 and E110G cladding tubes

M. Király*, Z. Hózer, M. Horváth, T. Novotny, E. Perez-Feró, N. Vér

Hungarian Academy of Sciences Centre for Energy Research, Fuel and Reactor Materials Department, P.O. Box 49, Budapest, H-1525, Hungary

ARTICLE INFO

Article history:
Received 23 August 2018
Received in revised form
25 October 2018
Accepted 2 November 2018
Available online 2 November 2018

Keywords:
E110
E110G
Tensile test
Tensile strength
Heat treatment
Oxidation
Hydrogenation

ABSTRACT

The mechanical and corrosion behavior of the Russian zirconium fuel cladding alloy E110, predominantly used in VVERs, has been investigated for many decades. The recent commercialization of a new, optimized E110 alloy, produced on a sponge zirconium basis, gave the opportunity to compare the mechanical properties of the old and the new E110 fuel claddings.

Axial and tangential tensile test experiments were performed with samples from both claddings in the MTA EK. Due to the anisotropy of the cladding tubes, the axial tensile strength was 10–15% higher than the tangential (measured by ring tensile tests). The tensile strength of the new E110G alloy was 11% higher than that of the E110 cladding at room temperature.

Some samples underwent chemical treatment – slight oxidation in steam or hydrogenation – or heat treatment – in argon atmosphere at temperatures between 600 and 1000 °C. The heat treatment during the oxidation had more significant effect on the tensile strength of the claddings than the oxidation itself, which lowered the tensile strength as the thickness of the metal decreased. The hydrogenation of the cladding samples slightly lowered the tensile strength and the samples but they remained ductile even at room temperature.

1. Introduction

A number of studies have examined the mechanical and oxidation properties of cladding materials, mainly Western zirconium alloys with high tin content like Zircaloy-2 and Zircaloy-4. Today, these alloys are being replaced by improved ones containing less tin, for example ZIRLO (Zr–Sn–Nb–Fe) and M5 (Zr-Nb-Fe) [1]. The fuel cladding alloy currently used in VVER-type nuclear power plants is the relatively well-known E110 Zr1%Nb alloy. Recently, many new variants have been introduced, like the E110G Zr1%Nb alloy based on a different raw material. At the request of Paks Nuclear Power Plant the Hungarian Academy of Sciences Centre for Energy Research (MTA EK) initiated a research program to establish the mechanical properties of the new E110G alloy in comparison with the currently used E110 alloy [2,3].

The zirconium for the E110 cladding alloy – currently used in Paks NPP – is manufactured via the iodide and the electrolytic processes [4]. In the iodide method the gaseous zirconium tetraiodide (ZrI_4) is condensed on a narrow tungsten filament and it thermally decomposes, whereby the zirconium metal is deposited on the tungsten (van Arkel – de Boer procedure). During the electrolytic process potassium-hexafluoro-zirconate ($K_2[ZrF_6]$) is mixed with molten salts (e.g. KCl, NaCl) and the zirconium precipitates from the melt onto the electrode surface. Like Western nuclear fuel manufacturers, the Russian supplier also develops the cladding materials. One such improvement is to convert from the former electrolytic procedure to sponge technology (Kroll process), used predominantly in the West. The essence of this process is that zirconium-tetrachloride is reduced with magnesium and then the magnesium is evaporated from the metal in vacuum. The new E110G cladding (G stands for Russian sponge, *gubka*) contains zirconium metal coming from the sponge process, which is sometimes mixed with metal from the iodide process [3,4]. The manufacturing process is the same for both alloys, β-forging and water quenching (1050 °C), then pressing, cold rolling and final recrystallization anneal in the α-region (560–620 °C) [5].

It is difficult to give the chemical composition of the E110G alloy. Our own measurements performed with a spark source mass spectrometer [2] are shown it Table 1. The results are similar to the composition specified by the manufacturer. However, we couldn't measure the light elements, so the amount of two important

* Corresponding author.
E-mail address: kiraly.marton@energia.mta.hu (M. Király).

https://doi.org/10.1016/j.net.2018.11.002

Table 1
Measured elemental composition of the E110 and E110G alloys in weight ppm (zirconium content is the balance 99 wt%).

Material	Nb	Mg	Al	Si	Cr	Mn	Fe	Ni	Cu	Hf
E110	10000	0.5	0.5	1	10	0.1	45	15	0.5	100
E110G	10000	1.5	10	35	30	5	500	15	5	10

elements (O and F) is unknown. In the literature the oxygen content for E110 was given as below 1000 ppm, typically between 500 and 700 ppm [6], for E110G 840 ppm of oxygen is reported [7]. The fluorine content is typically below 10 ppm, but it is significant as it may have strong effects on the oxidation behavior [8]. The E110G alloy has lower total impurity content [4], especially hafnium, and has a noticeably higher iron content, probably as a means to lower the corrosion and the creep rate. A combination of these factors has a positive effect on the embrittlement of the claddings [4,9,10].

This paper is an overview of the research activities conducted in MTA EK between 2012 and 2017 regarding the mechanical properties of these Russian zirconium cladding alloys. The purpose of the majority of this research was to assess the differences between these alloys and to determine the ultimate tensile strength of as-received, chemically and thermally treated E110 and E110G cladding tubes.

2. Experimental

2.1. Tensile testing geometry

We performed axial and tangential ultimate tensile strength (UTS) measurements to determine the anisotropy of the cladding tubes. The geometry of both cladding types was 9.1 mm outer dimeter with wall thickness of 0.65 mm, the surface of the tubes was polished. A new sample geometry had been chosen for the axial tensile testing based on foreign literature (Fig. 1.), along the lines of those used in RIAR in Dimitrovgrad [11]. For the measurement of the tangential tensile strength of the claddings the dies (two semicircles with the diameter of 7.5 mm) used in a similar research program in AEKI (predecessor of MTA EK) were used [12]. The tangential tests were carried out using 2 mm wide rings. Beforehand, Finite Element Modelling was used to evaluate if these geometries are applicable for UTS measurements and the result were favorable [13]. The ring samples were prepared from the cladding tubes by slow cutting, the axial samples were prepared by CNC (computer numerical control) milling to achieve sample uniformity.

2.2. Experimental design matrices

Two test matrices were constructed with respect to the rules of experimental design as well as the amount of available cladding tubes. The first design was constructed to determine the axial and tangential UTS of the as-received and chemically treated (oxidized or hydrogenated) cladding samples. The axial and ring tensile test

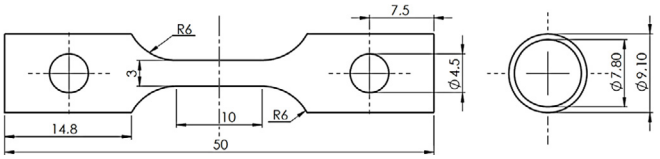

Fig. 1. Drawing of the machined two-winged axial tensile test samples. Dimensions are given in millimeters.

were carried out at room temperature, at an elevated temperature (150 °C) and near the expected operating temperature (at 300 °C) with cladding samples of both alloys. The ring and axial tensile tests were carried out using an Instron 1195 universal testing machine fitted with a custom-built furnace. The crosshead speed was 0.5 mm/s in all measurements. This corresponds to 5%/min strain rate for the axial and 4.1%/min strain rate for the ring samples.

Tensile tests of 15 axial and 63 ring samples for each alloy were conducted in this series. In order to reduce the amount of cladding tubes used, only the ring test were conducted at all the points of the experimental design, with three parallel measurements. The axial samples were tested only at certain points and only two parallel tests were conducted. The sample geometry and the load-displacement curve was registered and the ultimate tensile strength was calculated from the maximal force and the original cross section at the middle of the samples.

In the second experimental series we wanted to determine the effect of various heat treatments on the ultimate tensile strength of the E110 and E110G cladding rings and to assess the differences between the effects of the heat treatment and the high temperature oxidation in steam. In order to achieve this goal, ring tensile experiments were carried out at room temperature on as-received, heat treated and oxidized E110 and E110G alloy rings in 2015. The test matrix was constructed to investigate the effects of various heat treatments (600–1000 °C) on the ultimate tensile strength of the claddings. To be able to separate the effects of the oxidation from the effects of the heat treatment, the time and temperature of the heat treatment was equivalent to the chemical treatment of the previously oxidized samples.

Tensile tests of 81 ring samples for each alloy were conducted in this series. 6 ring tensile tests were performed for each treatment time, each temperature and each alloy, 3 of these were oxidized and 3 were heat treated samples. The sample geometry and the load-displacement curve was registered and the ultimate tensile strength was calculated. The E110 samples oxidizes at 800 °C for 2430 s suffered breakaway oxidation and were ultimately left out of the evaluation as the remaining wall thickness couldn't be measured.

2.3. Sample preparation

To test the effects of the corrosion and other changes that might happen to the cladding during normal operation, the experimental program included samples with moderate oxidation in steam and moderate hydrogen uptake relevant to normal operation conditions to evaluate how these chemical treatments affect the mechanical properties of the claddings. Based on the first results the effect of high temperature annealing (heat treatment) was also investigated.

The purpose of the pre-oxidation of the tensile samples was to produce specimens with different oxide layer thicknesses for the tensile tests. During the first preliminary tests the ring samples were oxidized at 900 °C, but the E110 samples experienced breakaway oxidation at 3 ECR% (equivalent cladding reacted) and so we couldn't prepare the samples needed for the experimental design. The maximum oxidation was determined at 2.8 ECR% to avoid breakaway oxidation and to keep the surface of the samples intact. This was below the limit of the ductile-brittle transition for both alloys. The tensile samples were oxidized in high temperature (800 °C) steam-argon mixture (88: 12 V/V%) under isothermal conditions. To ensure the same oxidation conditions for the parallel measurements, four ring samples were oxidized simultaneously. The oxidation ratio was calculated from the weight gain of the samples as follows (1):

$$ECR\% = \frac{M_{Zr} \cdot \Delta m}{M_{O_2} \cdot m_0} \cdot 100 \quad (1)$$

M_{Zr} – molar weight of zirconium (91.24 g/mol),
M_{O_2} – molar weight of oxygen (2·16.0 g/mol),
m_0 – weight of the sample before oxidation (mg),
Δm – weight increase of the sample after oxidation (mg).

To achieve the oxidation rate of 1, 2 and 2.8 ECR% for E110, the oxidation at 800 °C lasted for 360, 1500 and 3700 s, and for E110G it was 260, 1050 and 2430 s, respectively. The target oxidation was achieved with very high accuracy, with an average deviation of 0.03 ECR%. These samples were subjected to randomization prior to tensile tests so that the average oxidation rate of the three parallel ring samples selected for each tensile test temperature was approximately the same as that of the oxidation degree of all the samples in their category.

After additional tensile testing we found that the tensile strength of the ring samples prepared at 900 °C was significantly higher than that of the ring samples oxidized to the same ratio at 800 °C. This was due to the heat treatment the samples endured during the chemical treatment. During high temperature oxidation the zirconium alloys can undergo recrystallizing heat treatments, especially over the phase transition temperature range of 750–900 °C. This observation led to the foundation of the second design matrix. The heat treatment was conducted in inert argon gas atmosphere in the same apparatus as the oxidation. The mass gain of these samples due to air or steam ingress was kept under 0.1 wt%.

Hydrogen absorbed in the zirconium cladding leads to embrittlement, which can make it prone to cracking [14]. Hydrogen is at first dissolved in atomic form, at low concentrations it is soluble in zirconium. The beta zirconium can absorb more hydrogen, but this phase is stable only at higher temperatures. The alpha zirconium can dissolve only a limited amount; the maximum hydrogen content without precipitation is 700 ppm at 550 °C [15]. By further increasing the hydrogen content or by lowering the temperature, phase conversion (hydride formation) can occur and the Zr_2H_3 phase will emerge. Cooling hydrogenated zirconium from elevated temperatures will precipitate hydrides in the metal forming hydride plates.

The hydrogenation of the alloys E110 and E110G was conducted as follows. A three-zone tube furnace was fitted with a calibrated gas intake system and a vacuum system. Before the sample preparation was started, the heating element casings were degreased with an organic solvent (acetone) and then air-dried. The mass of the samples was weighed on the Sartorius SE2 Electronic Micro Balance scales. At the same time, four rings of the same alloy were placed on a quartz glass sample holder. In front of the ring samples 8 mm wide ring was placed in order to protect the samples from oxidation by air and water vapor possibly entering in the furnace.

After the furnace reached 600 °C and after multiple vacuuming the system was filled with high purity (99.999%) hydrogen up to the calculated initial pressure, and the pressure of the system was also supplemented with high purity (99.999%) argon to atmospheric pressure. The pressure for the total volume (hydrogen + argon) was continuously measured, the process of hydrogen absorption was indicated by a decrease in pressure. The time required for filling the samples with a certain amount of hydrogen was determined based on the previous test measurements. The pressure no longer decreased after 22 h of treatment as the hydrogen content of the zirconium rings was in equilibrium with the hydrogen in the tubes.

For each ring sample, the hydrogen content was calculated based on the weight gain. Blank tests were performed to determine the mass increase of the samples without the introduction of hydrogen, the contamination (mainly residual air and water) remained constant resulting about 60 ppm weight increase. The average weight gain of the blank test rings was deducted from the weight gain of the sample rings to estimate the hydrogen absorption accurately. Preliminary tests showed that the hydrogen content determined through hot extraction correlates well with the value calculated from weight gain. The target hydrogen content was achieved by on average 20 ppm accuracy. Samples were subjected to randomization prior to the tensile tests such that the average hydrogen content of the three parallel ring samples selected for each tensile test temperature was approximately the same as the average hydrogen content of the respective hydrogenation category.

3. Results

The ultimate tensile strength of each sample calculated from the average cross section and the measured maximal force. The total strain is calculated based on the length of the 10 mm long narrowed region for the axial samples and the original inner circumference of 24.5 mm for the rings. The results are shown in Table 2 for the axial and in Table 3 for the tangential tests of the first experimental design matrix and in Table 4 for the heat treated and in Table 5 for the oxidized samples of the second experimental design matrix. The effects of each variable (factor) was analyzed using analysis of variance (ANOVA). The dependent variable was the calculated tensile strength of the samples, and the factors were the sample material (E110 or E110G), the direction of tensile test (axial or tangential), the test temperature (20 °C, 150 °C, 300 °C), as well as the time, temperature and type of the treatment (in argon, steam or hydrogen). The factorial variance analysis calculates statistically detectable deviations of mean values for each level of the variables, and whether the different levels of a given factor change the expected value of the measured points, or it was only random error and standard deviation. Due to the large number and the interlinking distribution of the factors, the data was divided into several parts so that for example the effects of the temperature and the testing direction could be examined separately from the effects of the chemical treatments.

StatSoft STATISTICA 10 program was used to perform the variance analysis. Since the true degree of oxidation of the samples and the amount of hydrogen absorbed in them were in good agreement with the values set out in the experimental design, we used these categories in the analysis of variance instead of the exact measured values. The values on the horizontal axis of the charts produced are the different levels of the factors, not the exact values. Level 0 represented blank (heat treated) samples, separate from the untreated, as-received samples.

3.1. Evaluation of the effect of the testing temperature and direction

The first factorial ANOVA test was performed using the calculated tensile strength of 30 as-received samples; the results are illustrated in Fig. 2 and Fig. 3. The probability that the given effect is generated by random error indicates if the effect that has a significant effect on tensile strength at a 95% confidence level, assuming normal distribution. All three factors have a significant effect on tensile strength, the largest of which is the effect of the test temperature. With the increase in temperature, the tensile strength of the alloys is significantly reduced. The collected data shows that there are significant differences between the two alloys tested.

The direction dependence of the UTS can also be observed, the

Table 2
The first experimental design matrix with the average axial ultimate tensile strength and the total strain of the E110 and the E110G samples at different temperatures.

Sample preparation		Temperature of mechanical testing	Axial tests			
			Average UTS (MPa)		Average total strain (%)	
			E110	E110G	E110	E110G
As received		20 °C	408	457	49	50
Oxidized	1 ECR%		–	–	–	–
	2 ECR%		433	467	29	34
	2.8 ECR%		–	–	–	–
Hydrogenated	100 ppm		–	–	–	–
	250 ppm		383	436	32	36
	400 ppm		–	–	–	–
As received		150 °C	311	336	54	55
Oxidized	1 ECR%		–	–	–	–
	2 ECR%		335	353	35	48
	2.8 ECR%		–	–	–	–
Hydrogenated	100 ppm		–	–	–	–
	250 ppm		285	296	54	61
	400 ppm		–	–	–	–
As received		300 °C	227	236	49	58
Oxidized	1 ECR%		250	270	41	44
	2 ECR%		277	287	30	27
	2.8 ECR%		268	300	26	29
Hydrogenated	100 ppm		197	202	51	55
	250 ppm		201	210	48	51
	400 ppm		217	226	45	48

Table 3
The first experimental design matrix with the average tangential ultimate tensile strength and the total strain of the E110 and the E110G samples at different temperatures.

Sample preparation		Temperature of mechanical testing	Tangential tests			
			Average UTS (MPa)		Average total strain (%)	
			E110	E110G	E110	E110G
As received		20 °C	361	405	20	19
Oxidized	1 ECR%		345	398	24	24
	2 ECR%		357	402	22	22
	2.8 ECR%		363	406	20	20
Hydrogenated	100 ppm		332	395	24	23
	250 ppm		349	382	24	25
	400 ppm		341	374	24	25
As received		150 °C	262	282	27	27
Oxidized	1 ECR%		262	290	25	26
	2 ECR%		275	291	25	25
	2.8 ECR%		283	310	23	24
Hydrogenated	100 ppm		245	281	28	27
	250 ppm		252	284	27	28
	400 ppm		249	271	29	29
As received		300 °C	194	193	26	27
Oxidized	1 ECR%		211	224	25	26
	2 ECR%		220	226	25	25
	2.8 ECR%		226	234	24	24
Hydrogenated	100 ppm		182	194	27	26
	250 ppm		184	190	25	26
	400 ppm		194	193	26	28

tangential tensile strength determined by the ring tensile tests is lower than the axial tensile strength. The average axial ultimate tensile strength at ambient temperature was 408 MPa for E110 and 457 MPa for E110G samples. During the tensile test the two wings of the machined axial specimens elongated symmetrically and tore at almost the same loads, which supported the results of the previous finite element modelling. The tangential ultimate tensile strength of the as-received E110 and the E110G ring samples was different, 361 MPa for E110 and 405 MPa for E110G. For both alloys the ultimate tensile strength in the tangential direction was 10–15% lower than the axial ultimate tensile strength. The UTS of the E110G cladding samples was for 11% higher than that of the E110 samples in both axial and tangential direction, although this difference was smaller for higher temperatures.

Furthermore, two cross effects were significant, one between the temperature and the alloy and another between the temperature and the direction. In other words, the difference between the UTS of the two alloys tested in two directions was somewhat dependent on the temperature. These effects were smaller than the main effects of the factors, but were shown to be significant in our analysis.

3.2. Evaluation of the effect of heat treatment temperature and time

From the results of the second experimental design we determined the effect of heat treatment in inert atmosphere and again significant differences were found between the two alloys (Fig. 4.). This may hint at the different crystal structures and heat treatments

Table 4
The second experimental design matrix of ring tensile tests with the average tangential ultimate tensile strength and the total strain of the heat treated E110 and E110G samples measured at room temperature.

Treatment temperature (°C)	Treatment time (s)	Ring samples heat treated in argon			
		Average UTS (MPa)		Average total strain (%)	
		E110	E110G	E110	E110G
600	1050	340	406	25	26
	3700	342	411	25	27
	7200	347	410	24	26
700	1050	369	418	25	26
	3700	361	417	23	26
800	360	–	–	–	–
	1050	381	413	27	26
	1500	385	419	25	26
	2430	391	423	25	25
	3700	408	428	21	24
900	280	427	443	24	26
	390	426	446	23	25
	690	426	449	23	25
	2430	433	446	23	25
1000	280	449	442	20	23
	690	472	459	23	22
	3700	563	489	20	19

Table 5
The second experimental design matrix of ring tensile tests with the average tangential ultimate tensile strength and the total strain of the oxidized E110 and E110G samples measured at room temperature.

Treatment temperature (°C)	Treatment time (s)	Ring samples oxidized in steam					
		Oxidation ratio (ECR%)		Average UTS (MPa)		Average total strain (%)	
		E110	E110G	E110	E110G	E110	E110G
600	1050	–	–	–	–	–	–
	3700	–	–	–	–	–	–
	7200	0.6	0.7	331	410	26	26
700	1050	–	–	–	–	–	–
	3700	1.5	1.7	337	398	24	25
800	360	1.0	1.2	345	398	24	24
	1050	1.8	2.0	361	402	23	22
	1500	2.1	2.6	357	388	22	24
	2430	2.7	2.8	370	406	21	20
	3700	2.8	3.6	363	416	20	21
900	280	1.8	2.0	399	436	21	23
	390	2.0	2.6	409	472	20	22
	690	2.9	3.1	404	479	18	18
	2430	–	5.0	–	473	–	17

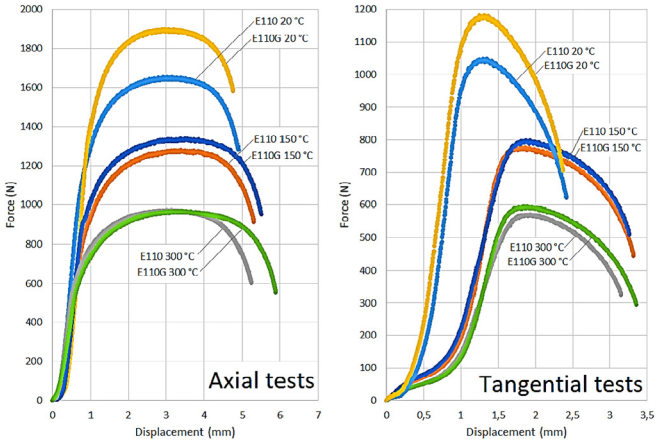

Fig. 2. Load-displacement curves of some axial (left) and tangential tensile tests (right) of as-received E110 and E110G samples measured at different temperatures.

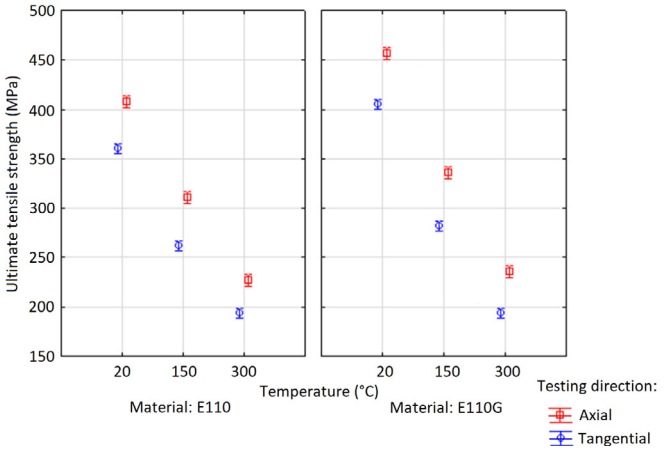

Fig. 3. The axial and tangential ultimate tensile strength of the as-received E110 and E110G samples measured at three temperatures.

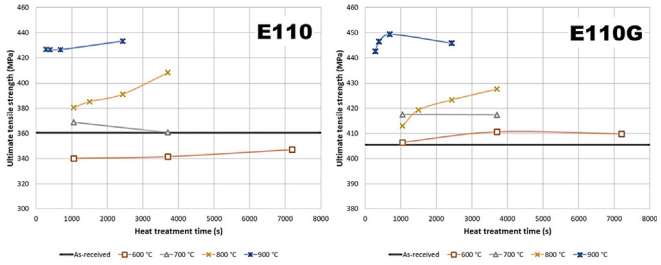

Fig. 4. The ultimate tensile strength of E110 (left) and E110G (right) ring samples at ambient temperature, after different heat treatments, compared to the ultimate tensile strength of as-received samples. The axis is different on the two diagrams as the extent of the change in the UTS is different.

of these two claddings.

The heat treatment itself had a significant effect on the tensile strength of the zirconium alloys. Heat treatment at 600 °C led to the softening of E110 tubes, and the tensile strength of the samples decreased by an average of 5%. At this temperature, the diffusion of atoms in the crystal leads to the decrease of the number of dislocations and so the hardness of the alloy decreases as well. This process was not observed regarding the E110G samples, which suggests that the new alloy tubes received a more perfect stress relief annealing than the E110.

The heat treatments over 700 °C raised the tensile strength of the samples. During heat treatment at 800 °C, the alloys began to harden, as above 750 °C the phase transition of zirconium starts and the hexagonal close-packed α phase stable at lower temperatures is transformed into the body-centered cubic β phase developing needle-shaped crystals. Measurements at this temperature showed the importance of the length of the heat treatment, as longer treatment time led to greater phase change, and so the UTS was higher. After an hour of heat treatment at 800 °C the tensile strength of E110 increased by 10–15% compared to the as-received samples, this was only 5% for E110G. During the heat treatment at 900 °C the phase transformation happens quickly and completely, thus the length of the heat treatment had no significant effect. The UTS of E110 increased 20%, while for E110G this was 10%.

3.3. Evaluation of the effect of the oxidation in steam separately from the heat treatment

In the experimental design all samples oxidized in high temperature steam had a counterpart, a heat treated sample treated in pure argon for the same time and at the same temperature as the oxidation. The design was set up this way to separate the UTS modifying effect of the high temperature oxidation and the heat treatment. Data showing the relationship between the treatment temperature and the tensile strength is seen in Fig. 5, the averages and the 95% confidence intervals were depicted. It can be seen that the oxidation has a negative effect on the tensile strength of the cladding tubes. The calculated tensile strength of the oxidized samples is mostly under the heat treated samples by 5–10%.

The effect of the oxidation in steam on the tensile strength of the samples was relatively minor compared to the effect of the heat treatment in inert atmosphere. The effect of oxidation on the tensile strength was found to be slightly negative, as the tensile strength of oxidized samples were on average 5% lower than the heat treated ones. This measurement series implies that the effect of the heat treatment on the UTS during high temperature oxidation is comparable to the effect of the oxidation itself. For example the slightly increased tensile strength after oxidation in steam atmosphere at 800 °C appears to be the combination of the positive

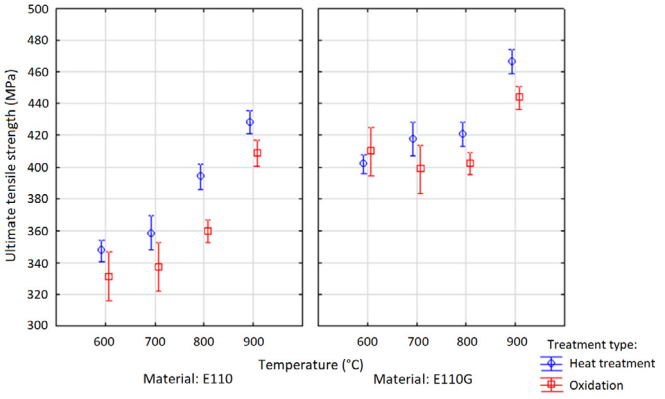

Fig. 5. The tangential ultimate tensile strength of the heat treated (690 s or 1050 s) and the oxidized E110 and E110G samples measured at room temperature.

effect of the heat treatment (increasing with the treatment time) and the slightly negative effect of the oxidation in steam.

Since the experimental plan was partial (i.e. not every treatment time was used for all temperatures), the statistical evaluation (ANOVA) could only be done for 800 °C and 900 °C (Fig. 6.). The difference between the heat treated and the oxidized samples was significant. The effect of oxidation on the tensile strength was very small, at the limit of statistical detection as the inherent variance of the data was high.

The 5% measured increase in tensile strength is comparable to the accuracy of our measurements. Based on the data we estimated the relative standard deviation. For a total of 166 data points it was on average 2.24%, but in certain cases it was close to 7%. This error is mainly due to the imperfect measurement of the geometry of the ring samples (mainly due to burr on the edges), and in many cases the uneven surface of the oxidized samples. 0.04 mm uncertainty in the average wall thickness of the rings may cause 5% deviation in the calculated tensile strength.

3.4. Evaluation of the hydrogenation

The effect of the hydrogenation (100, 250, 400 wt ppm absorbed hydrogen) affecting the tensile strength appears to be very small. We attempted to separate the effects of the hydrogenation from the effect of the heat treatment during the production of the samples, using the results of the tensile tests of blank samples that were heat treated at 600 °C for 22 h similarly to the hydrogenated samples.

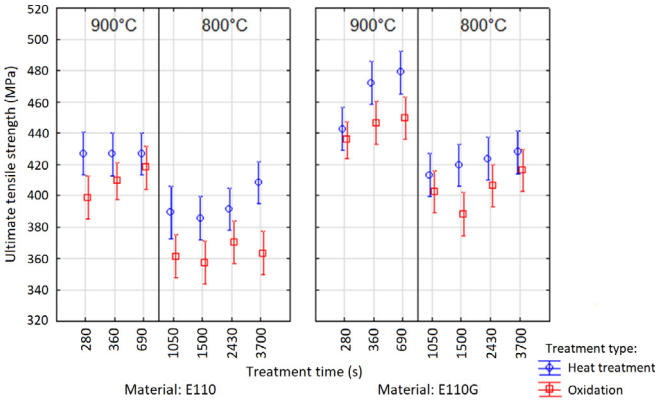

Fig. 6. The tangential ultimate tensile strength of the 800 °C and 900 °C heat treated and the oxidized E110 and E110G samples versus the treatment times, measured at room temperature.

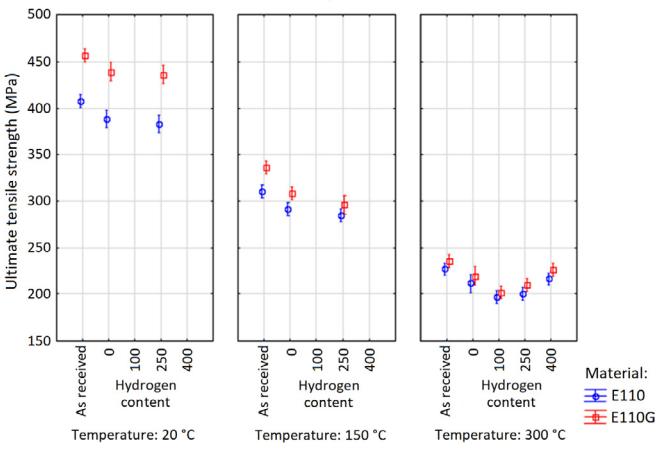

Fig. 7. The axial ultimate tensile strength of the hydrogenated E110 and E110G samples measured at three temperatures.

The points shown in Fig. 7 and Fig. 8 (Level 0 is referring to the heat treated blank samples here) are close to the main effect, i.e. the effect of the hydrogen is at the boundary of statistical detectability. The effect is only visible in the case of larger quantity (≥250 ppm) of hydrogen addition. For the whole examined range it can be seen that hydrogenation slightly reduces tensile strength. The effect of hydrogenation measured at room temperature was found to be significant in the examination with less than 1% probability that this effect was only due to the uncertainty due to normal distribution (at 95% confidence level). The absorption of 250–400 ppm of hydrogen reduces the tensile strength of the investigated zirconium alloys by 10 MPa. This effect was not detectable at higher temperatures.

4. Discussion

The main goals of the research were achieved: the mechanical properties of the two Russian cladding alloys were evaluated and compared, the anisotropy of the cladding materials was demonstrated, the effects of the chemical treatments were assessed and were separated from the effects of the heat treatment. The standard deviation of the tensile tests was quite high, even though three parallel measurements were made, and therefore the UTS could only be calculated with 3% relative error.

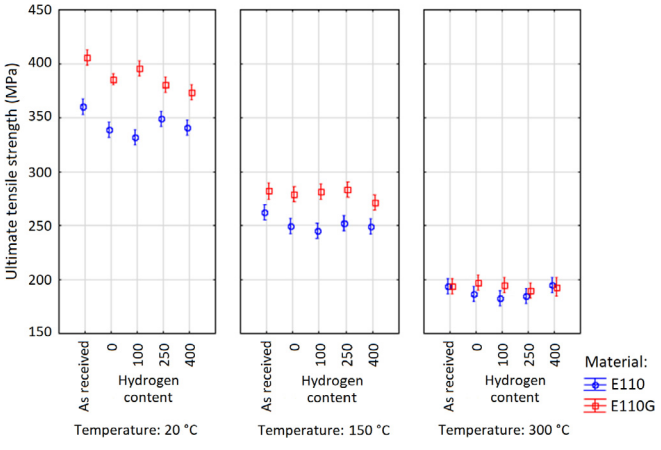

Fig. 8. The tangential ultimate tensile strength of the hydrogenated E110 and E110G samples measured at three temperatures.

Table 6
Axial/Tangential UTS quotient for as-received samples.

Testing temperature	E110	E110G
20 °C	1130	1128
150 °C	1187	1191
300 °C	1170	1223

Table 7
The axial UTS values found in the literature for the E110 alloy at 25 °C and at 300 °C.

Publication (date)	UTS (MPa) at 25 °C	UTS (MPa) at 300 °C
Thorpe and Smith (1978) [16]	393	200
Nikulina et al. (1996) [17]	380	209
Vesely et al. (1998) [18]	407	–
Kaplar et al. (2001) [19]	378	–
AEKI (1999) [12]	371	240
MTA EK (current)	408	227

The two tested cladding alloys differed substantially. Both the axial and the tangential UTS calculated for the E110G alloy samples was on average 11% higher than for the E110 samples. For both alloys the UTS in the hoop direction was more than 10% lower than the axial UTS. This was attributed to the anisotropy of the cladding material. The quotient of the axial and tangential UTS is similar for both alloys, and seems to depend on the temperature, as seen in Table 6.

Our calculated 408 MPa average UTS for the axial E110 samples is in good agreement with the data available in various other databases. These measurements were conducted using either cladding tubes or flattened, standardized tensile samples, measured in the axial direction. The difference among the UTS calculated from the testing of the various sample geometries could be attributed to the method of sample preparation, the heat treatment, surface oxidation and the work hardening of the samples during cutting and machining. The difference could also be attributed to the changes in the manufacturing process of E110 over the years. The values found in the literature are collected in Table 7.

5. Conclusions

Numerous experiments have been conducted in MTA EK in the last few years regarding the mechanical testing of Russian zirconium cladding alloys. The purpose of the presented research was to determine the ultimate tensile strength of E110 and E110G cladding tubes at room temperature and higher temperatures, and to assess the differences between these alloys. The tensile tests were conducted using machined axial and ring cladding samples, some of them were slightly oxidized or hydrogenated.

Tensile test experiments were performed with samples from both claddings, these included axial and tangential tensile tests at 20, 150 and 300 °C. Some samples underwent chemical and heat treatments, and the effects of these were evaluated. The chemical treatments were slight oxidation in steam at 800 °C for up to 2.8 ECR%, or hydrogenation at 600 °C up to 400 ppm, the heat treatment was in argon atmosphere at temperatures between 600 and 1000 °C. These samples were tested at room temperature.

The direction dependence of the UTS was observed, the tangential tensile strength determined by the ring tensile tests was lower than the axial tensile strength. For both alloys the ultimate tensile strength in the tangential direction was 10–15% lower than the axial ultimate tensile strength. The UTS of the E110G cladding samples was 11% higher than that of the E110 samples in both axial and tangential direction, although this difference was smaller for higher temperatures.

Heat treatment at 600 °C led to the softening of E110 tubes, and the tensile strength of the samples decreased by an average of 5%, however, this was not observed regarding the E110G samples. The heat treatments over 700 °C raised the tensile strength of the samples. During heat treatment at 800 °C, the alloys began to harden, treatments at this temperature showed the importance of the length of the heat treatment, as longer treatment time led to greater phase change, and so the UTS was higher. The UTS of E110 increased by 20%, while for E110G this was 10%.

The effect of the oxidation in steam on the tensile strength of the samples was relatively minor compared to the effect of the heat treatment in inert atmosphere. The effect of oxidation on the tensile strength was found to be slightly negative, as the tensile strength of the oxidized samples were on average 5% lower than the heat treated ones. The effect of the heat treatment on the UTS during high temperature oxidation was comparable to the effect of the oxidation itself. The absorption of 400 ppm of hydrogen reduces the tensile strength of the investigated zirconium alloys by 10 MPa. This effect was not detectable at higher temperatures.

Conflict of interest

There is no conflict of interest in the funding and the publication of this research.

Acknowledgments

The research activities presented were funded by Paks NPP (contract number: 4000040339 EK-G-1112/2013) and the National Research, Development and Innovation Fund of Hungary (contract number: NVKP_16-1-2016-0014).

References

[1] J.P. Mardon, D. Charquet, J. Senevat, M. Griffiths, B.D. Warr, A. Stasser, J.R. Theaker, H. Rosenbaum, B. Cheng, Influence of composition and fabrication process on out-of-pile and in-pile properties of M5 alloy, in: Zirconium in the Nuclear Industry: 12th International Symposium, STP1354, 2000, pp. 505–523.

[2] E. Perez-Feró, T. Novotny, Z. Hózer, M. Kunstár, High temperature oxidation experiments with sponge base E110G cladding, in: Proceedings, 10th International Conference on WWER Fuel Performance, Modelling and Experimental Support, 7-14 September, Sandanski, Bulgaria, 2013. ISSN 1313-4531.

[3] Z. Hózer, E. Perez-Fero, T. Novotny, I. Nagy, M. Horváth, A. Pintér-Csordás, A. Vimi, M. Kunstár, T. Kemény, Experimental comparison of the behavior of E110 and E110G claddings at high temperature, in: Zirconium In The Nuclear Industry: 17th International Symposium, STP1543, 2015, pp. 932–951.

[4] S.A. Nikulin, A.B. Rozhnov, V.A. Belov, E.V. Li, V.S. Glazkina, Influence of chemical composition of zirconium alloy E110 on embrittlement under LOCA conditions— Part 1: oxidation kinetics and macrocharacteristics of structure and fracture, J. Nucl. Mater. 418 (2011) 1–7.

[5] P. Rudling, R.B. Adamson, Zirat Special Topical Report on Manufacturing (Zirat-5), Advanced Nuclear Technology Sweden AB, ANT, 2000.

[6] P.V. Shebaldov, M.M. Peregud, A.V. Nikulina, Y.K. Bibilashvili, A.F. Lositski, N.V. Kuz'menko, V.I. Belov, A.E. Novoselov, E110 alloy cladding tube properties and their interrelation with alloy structure-phase condition and impurity content, in: Zirconium in the Nuclear Industry: 12th International Symposium, STP1354, 2000, pp. 545–559.

[7] J. Ríha, P. Sutta, Phase transformations of E110G Zr-alloy observed by “in situ” XRD, Mater. Struct. (Bulletin of the Czech and Slovak Crystallographic Association) 22 (2015) 82–85.

[8] V. A. Markelov, A. G. Malgin, V. V. Novikov, Providing durability in a LOCA design basis accident of fuel rod claddings made of electrolytic zirconium E110 alloy. Water Reactor Fuel Performance Meeting, 10-14 September 2017, Jeju Island, South Korea.

[9] S.A. Nikulin, A.B. Rozhnov, A.Yu Gusev, T.A. Nechaykina, M.Yu Zadorozhny, Fracture resistance of Zr–Nb alloys under low-cycle fatigue tests, J. Nucl. Mater. 446 (2014) 10–14.

[10] A.V. Nikulina, V.F. Konkov, V.N. Shishov, M.M. Peregud, T.N. Khokhunova, N.Y. Gorskaya, L.P. Sinelnikov, O.A. Golosov, Interrelation of alloy composition of zirconium Nb-containing alloys with corrosion and mechanical properties, in: 7th Russian Conference on Reactor Material Science, Russian Federation, Dimitrovgrad, 2003.

[11] L. Yegorova, et al., Database on the behavior of high burnup fuel rods with Zr1%Nb cladding and UO2 fuel (VVER type) under reactivity accident conditions, NUREG/IA-0156 2 (July 1999).

[12] A. Griger, L. Maróti, L. Matus, P. Windberg, Ambient and High Temperature Mechanical Properties of ZrNb1 Cladding with Different Oxygen and Hydrogen Content, Enlarged Halden Programme Group Meeting, 24-29, Loen, Norway, May 1999.

[13] M. Király, D.M. Antók, M. Horváth, Z. Hózer, Evaluation of axial and tangential ultimate tensile strength of zirconium cladding tubes, Nucl. Eng. Technol. 50 (2018) 425–431.

[14] N.M. Vlasov, I.I. Fedik, Hydrogen embrittlement of zirconium alloys, Met. Sci. Heat Treat. 45 (2003) 328–331.

[15] M. Grosse, M. Steinbrueck, E. Lehmann, P. Vontobel, Kinetics of hydrogen absorption and release in zirconium alloys during steam oxidation, Oxid. Metals 70 (2008) 149–162.

[16] R. Thorpe, I.O. Smith, Tensile properties of Zr-wt1%Nb alloy, J. Nucl. Mater. 78 (1978) 49–57.

[17] A.V. Nikulina, V.A. Markelov, M.M. Peregud, Y.K. Bibiasvili, V.A. Kotrehkov, A.F. Lositsky, N.V. Kuzmenko, Y.P. Shevin, V.K. Shamardin, G.P. Kobylyansky, A.E. Novoselov, Zirconium alloy E635 as a material for fuel rod cladding and other components of VVER and RBMK Cores, in: Zirconium in the nuclear industry: 11th International Symposium, STP1295, 1996, pp. 785–804.

[18] J. Vesely, M. Valach, Z. Frejtich, V. Priman, Creep properties of non-irradiated ZrNb1 cladding tubes under normal and abnormal storage conditions, IAEA-Tecdoc 1089 (1998) 305–312.

[19] A. Kaplar, L. Yegorova, K. Lioutov, A. Konobeyev, N. Jouravkova, Mechanical properties of unirradiated and irradiated Zr-1% Nb cladding, NUREG/IA-0199 (2001).